



Intelligent Health Assistant for Pupils

Le Quang Thao^{1,2*}, Ngo Chi Bach², Pham Xuan Bach³, Le Phan Minh Hieu³, To Gia Phuc⁴

¹ Faculty of Physics, VNU University of Science, Hanoi 100000, Vietnam

² University of Science, Vietnam National University, Hanoi 100000, Vietnam

³ Hanoi-Amsterdam High School for the Gifted, Hanoi 100000, Vietnam

⁴ Reigate Grammar School of Vietnam, Hanoi 100000, Vietnam

Corresponding Author Email: thaolq@hus.edu.vn

<https://doi.org/10.18280/i2m.220102>

ABSTRACT

Received: 10 August 2022

Accepted: 19 October 2022

Keywords:

posture, proximity sensors, wireless sensor network, drowsy detect, correct posture

In recent years, pupils' health has been taken into consideration more than ever, and the raising of correcting posture in humans or specifically pupils posture was extremely noticeable. The purpose of this project is to propose a system using a wireless sensor network integrating a body tilt sensor, an infrared proximity sensor, a particle dust sensor, and a camera to detect children's drowsiness states using a neural-network-based facial landmark detection. The monitoring of children's posture operates based on their body movements and the distance of their eyes to the table, when the sensor detects an accepted limitation exceeding the parameter, the device will alert so that the pupils can reconfirm their sitting posture. We also created a website for remote tracking and saving data on children's posture. The accuracy and the effectiveness of the system has been verified by various experiments and give promising results. We expect that this system can be effective and easily operate so that people can utilize it to upgrade their quality of life.

1. INTRODUCTION

Human bones have the function to support the motor control and shape the form of the skeleton. Even though the bones only cover a part of the body's overall weight, it's strong enough to resist the force of the entire body [1]. Especially with examples of children's and teenager's spines, which they're smaller than those of adult's spines [2]. As a result, the human skeletal system also holds a vital function toward our general body's form. Because if the mechanism of the general bones structure is maintained securely and efficiently, the amount of effort to maintain the form would be greatly reduced. In contrast, if the skeletal system is not maintained effectively, especially the spines, the body will undergo significant damage [3, 4]. There are numerous causes of children's poor posture. Some kids' bags are too hefty to carry, which puts too much strain on their spine [5]. Additionally, excessive use of electronic gadgets that causes children to constantly gaze down at the screen and put a lot of strain on their neck muscles may result in poor posture [6, 7]. However, since young toddlers lack the capacity for recognition, they typically slouching on the table and adopt the bad habit of sitting incorrectly, which contributes to the presence of bad posture in many pupils [8, 9].

In this project, we concentrate on the final issue raised above and create a system that would aid kids in becoming more conscious of the proper sitting position and keeping it for extended periods of time. This objective prompted us to ask, "What variables contribute to poor seating habits and how to change them?". We investigated at five elementary schools in the vicinity of Ha Noi. There are around 5 to 7 classrooms in each grade at each school, with 40 to 50 kids in each class. The majority of the investigation was conducted through

observation and note-taking. We have come to the conclusion that there are two key reasons that kids having bad posture were that they hunch their backs so much when writing, and that two to four pupils always nod asleep during study time in each class. First of all, when studying, kids frequently decide to lie down on the table or hunch their backs which may lead to kyphosis [10]. This occurs because they don't need to exert a lot of power from the muscles around their spine to maintain such positions. On the contrary, certain muscle groups must constantly be in use to maintain proper posture, which first causes back weariness. Second, a lot of students doze off when studying, and this position interferes with the development of good posture. When youngsters fall asleep at the table, they frequently stoop and recline in a variety of positions, stretching their back muscles and weakening those muscles. Additionally, dozing off in class results in a reduction in student performance since learning is not fully retained [11].

In order to monitor and assist kids and reduce the harmful consequences of the aforementioned problems, we have incorporated four gadgets ranging in complexity from simple to advanced. First, we employ a Wireless Sensor Network (WSN) [12] to safeguard pupils' posture while studying. Based on theories from researches [13-15], this sensor network comprises a waist device with integrated sensors to track the inclination of children's lower back. It has been evident after several early tests that wearables alone are insufficient since many students frequently bow their heads at the table without bending their lower backs. To address this issue, we have further improved the system with a distance sensor [16] to measure distance between pupils faces to the table, which was also the concern in research [17]. This is done to make sure students are sitting up straight when studying and that their eyes are not too near to the table, which might lead to myopia

[18]. A camera with just enough resolution has been placed to address the issue of youngsters dozing off in class. We included a computer vision application called Facial Landmark Detection (FLD) [19] for the camera's software. This algorithm locates and monitors important facial landmarks, such as the spots around the nose, mouth, and eyes. The main processor will use the input from this algorithm to decide whether a youngster is ready to doze off then take the right action. Last but not least, we included a fine dust concentration monitoring device to keep an eye on the learning environment for the students. This idea was inspired by research [20, 21]. As our system is activated, if certain parameters of the particle matter [22] reach beyond a certain level, the student will receive a notification to clean the study space to ensure that it is a secure environment. The device also syncs, stores, and displays the system data, which parents may view on a straightforward webpage.

The following three sections comprise the presentation of our paper. The system's hardware, software, and finishing process are discussed in Part 1 - Materials and Methods. We also provide the system's operational algorithm in this section. Experiment and Result, Part 2 discusses real experiments that were conducted along with modifications to guarantee operational correctness. Finally, a conclusion is reached, and we provide recommendations for future research and development.

2. MATERIALS AND METHODS

2.1 System block diagram

Our project is separated into three stages, as seen in the Figure 1, and we continue to make major improvements throughout each step.

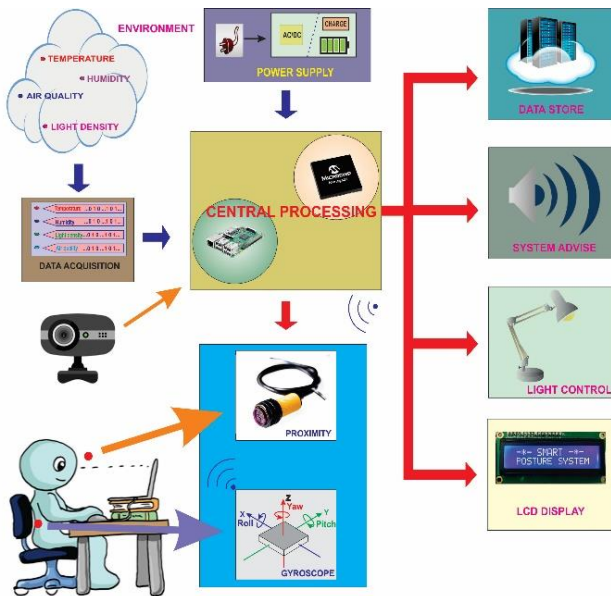


Figure 1. Diagram of the main block system

Our primary goal in the initial stage is to create wearable equipment that can motivate children to maintain a straight posture while studying. The mechanism of this device is straightforward: we install the tilt sensor unit MPU6050 [23], which is linked to the signal transmitter NRF24L01 [24]. These two components are frequently employed in several

applications which require high accuracy and effective information transfer such as [25]. The wearable gadget also has a direct connection to a vibrating mechanism that alerts the user when they are in the incorrect position. This vibrating element is made up of a tiny revolving shaft coupled to an eccentricity cylinder, which is similar to the vibrating motor that was implemented in research [26]. This device's setup steps are as follows: When the wearable unit and hub unit are both turned on, they immediately establish a 2.4 GHz wireless connection. After the user has worn the device and seated themselves properly, they press the setting button on the hub unit, this action will store the sensor's parameters at that moment and set them as the standard values. After that, users may securely sit and study. The wearable gadget will vibrate to notify them every time their lower back bends more than 15 degrees than the standard parameters, and it will cease once they have restored to the normal posture.

In order to enable the system to do two more distinct duties, we modified it for the following stage by adding a distance sensor and a fine dust sensor. We employ the GP2Y0A21YK0F sensor [27] as our distance sensor since it can measure lengths between 10 and 80 cm with an input voltage range of 4.5 V to 5 V, making it ideal for monitoring the distance between the user's head and the table while using less power. In order to accurately measure the distance from the table to the user's head, we proceed to put the sensor at the center unit and link it to the ATmega8 [28]. The sensor is tilted away from the table at an angle of 28.35 degrees (tai sao). When the user is using the device, the system will sound an auditory warning when the distance between the user's head and the sensor is less than 30cm [29], urging them to return to the proper posture. The system is then equipped with a fine dust sensor, model number GP2Y1010AU0F [30], to track the level of fine dust in the user's learning environment. The dust concentration characteristics are shown on the built-in Liquid Crystal Display (LCD) screen [31] by this sensor, which is also directly integrated with the center unit. The message: "Clean your area" will be shown on the LCD screen to alert users to clean their study space when the fine dust parameters reach the alarm threshold.

At the end of the project, we concentrated on developing a method for identifying drowsiness in youngsters as well as a website that would allow parents to keep tabs on their kids' status in the learning process. The system is equipped with an extra 8MP camera that is made specifically for use with the Raspberry Pi [32] and is combined with the FLD algorithm to achieve the former objective. Generally, FLD is a computer vision task that calls for the computer to identify facial landmarks like the eyes, nose, mouth, and points along the human facial skeleton [33, 34]. We included the Dlib library [35] - a widely used open source library that can recognize landmarks on human faces accompanying pre-trained Haar Cascade model to identify human faces [36, 37] in order for the software to be able to carry out those tasks. Despite the fact that both of these elements have been around for a while, they are still helpful in many projects today. For the latter objective, we have created a website with the server installed directly on the Raspberry Pi 3 according to the protocols which was similar to ref. [38] after finishing the hardware design and preparing for preliminary tests. This website enables parents to keep tabs on their children's progress during the learning process, including the length of time that kids maintain good posture and whether they nod asleep. These statistics are also shown as graphs for parents to monitor their child's progress.

2.2 Body tilt sensor

In our study, we employ the MPU6050 sensor, a type of sensor utilizing Microelectromechanical System (MEMS) [39] technology, to measure the deviation of pupils back. This sort of sensor was created by InvenSense's MotionFusion TM and includes both a 3-axis MEMS gyroscope and 3-axis MEMS accelerometer built inside it

2.2.1 MEMS-Accelerometer [40]

The change in capacitance is used by MEMS accelerometers to determine acceleration. It features exterior plates that are fixed and an attached mass that is attached to a spring that can only move in one direction. When acceleration is applied in a certain direction, the mass will move and the capacitance between the plates and the mass will vary. These capacitance variations will be detected, analyzed, and correlated with each specific acceleration value. Figure 2 demonstrates its microstructure.

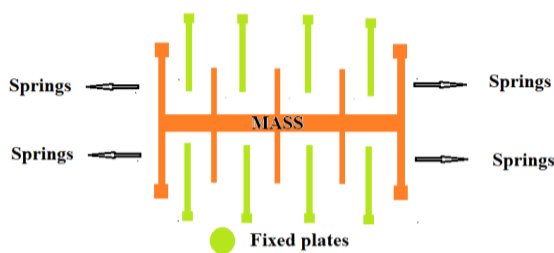


Figure 2. Principle working of MEMs accelerometers

2.2.2 MEMS-Gyroscope [41, 42]

The 3-axis micro-gyroscope device working on the Coriolis effect [9] as shown in Figure 3. It is made up of two fixed and two moveable microplastic frames that are joined together by springs that grow out of the micro capacitors. When the entire system is moving, the Coriolis force emerges and is perpendicular to the capacitor's plates. This results in a change in the capacitance value because the moving frame in the middle will no longer exclusively move in a direction parallel to the capacitor plates. This change in capacitance will be detected, analyzed, and correlated to a particular change in tilt angle, just like accelerometers do.

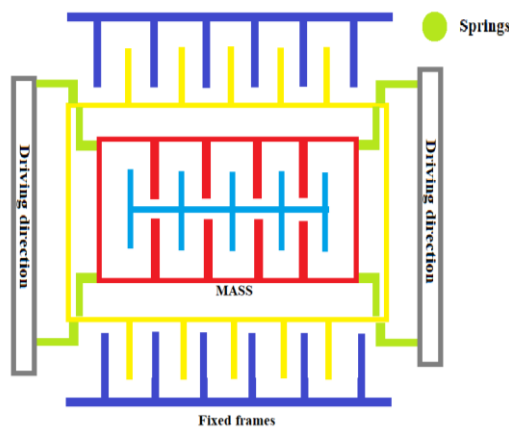


Figure 3. Principle working of MEMs gyroscope

When the gyro drift is taken into consideration, the platform system has an unstable component. In general, the combination of two factors- a slowly fluctuating, near-dc

variable called bias instability and a higher frequency noise variable termed angular random walk [43] is what causes the gyroscope to drift. The Kalman filter, which is how we resolve the issue, does provide an estimate of the gyro drift.

2.2.3 Kalman filter [44, 45]

One of the most significant and widely used estimate methods is the Kalman filter. It generates hidden variable estimations based on unreliable and erroneous measurements. As we have already introduced, the use of the tilt deviation measuring sensor presents us with two issues. The measurement's deviation from its average value of the output, which reveals how stable the gyro output is over time, is first defined as the bias instability. Otherwise, thermoelectric reactions are held accountable for the MEMS gyroscope's high frequency white noise. The Kalman filter uses previous estimation to forecast system output in order to address the aforementioned issues. In actual use, the MPU6050 will be in charge of monitoring children's posture and transmitting that information in real-time to our main device. The Kalman filter will forecast the next change based on how quickly the tilt changes whenever the kids move their bodies, then create the preferred data so that the impact of the inaccuracy is as little as possible

2.3 Particulate Matter (PM) dust sensor

Particles as small as 2.5 microns and 10 microns, which are too dark to be seen with the unaided eye, are examples of fine dust. They may penetrate deeply into children's lungs and cause major health issues, and they may even enter your bloodstream [46, 47]. One of the newest models in Sharp's line-up of PM dust sensors, the GP2Y1010AU0F operates on the concept of light scattering to detect and monitor the concentration of dust [48, 49].

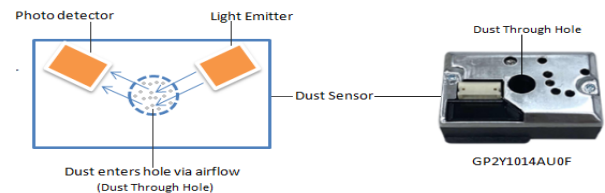


Figure 4. PM dust sensor principle working

Within the rectangular sensor package, there are holes on each side for dust coming through as shown in Figure 4, a photodetector and a Light Emitting Diode (LED) emitter that are set up in opposition to one another. When airborne dust enters the sensor chamber, it scatters the light from the LED emitter toward the photo-detector. The intensity of the dispersed light increases with the amount of dust in the air within the sensor chamber. The dust sensor produces a voltage value that fluctuates in accordance with the strength of the light that is scattered, which in turn reflects the amount of dust in the atmosphere. A linear relationship may then be used to get the real dust density from the output voltage value.

2.4 Particulate Matter (PM) dust sensor

A distance sensor is a dependable instrument for many applications that need accurate measurement, precise positioning, and the identification of a wide variety of

materials. We employ a GP2Y0A21YK0F [27] sensor in our project to measure the distance between students' heads and the table, which is made up of an IR LED and a light detector. It operates by utilizing the phenomena where an object's distance from the sensor may be determined by the infrared light beam's reflection off it. Using the triangulation principle as shown in Figure 5, the distance is computed [50].

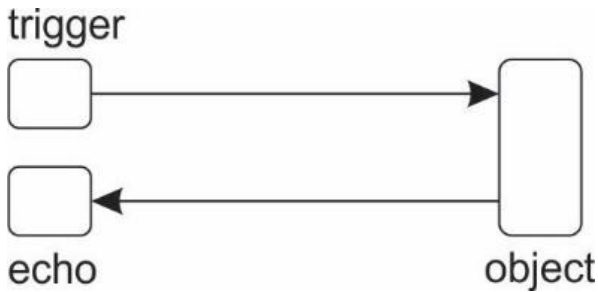


Figure 5. Path of IR beam

Distance can define by:

$$d = \frac{v \times t}{2} \quad (1)$$

where, v: velocity of the light in the air.

t: time for traveling from transmit signal to receive the feedback signal.

2.5 Communication module

Nordic Semiconductor's nRF24L01 [24] is a single-chip 2.4GHz transceiver with an integrated baseband protocol engine that has been upgraded with a ShockBurst hardware protocol accelerator that has a high-speed interface and minimal power requirements. Its range may go up to 100 meters when utilized in open space and at a lower baud rate.

2.6 Detect eyes and drowsiness

The system will recognize face landmarks in the input image from the camera in order to carry out the task of identifying drowsiness in youngsters. Areas around the eyes, mouth, nose, eyebrows, and facial skeleton were referred to as landmarks.

We incorporate the two libraries Dlib [35] and OpenCV [51] into the system to handle the two stages involved in setting up the landmarks discussed above. The camera will first gather the input student images, which are then processed by the built-in OpenCV-Haar Cascades algorithm [52-54], the benefit of this algorithm is that it can operate in real-time and recognize people in video streams. After that, an area defined by (x, y) coordinates is used to determine the identified face. The facial landmarks detector, which is part of the *dlib* package and first introduced by Kazemi and Sullivan [55]. It estimates 68 coordinates that stand in for facial landmarks on the face using a pre-trained dataset as shown in Figure 6.

Following the identification of these facial features, 12 points from 37 to 48 representing both eyes on the human face will be extracted. Since then, each eye is shown with 6 points. For the sake of clarity, we will refer to these six points in this

section as points 1, 2, 3, 4, and 5, these points are illustrated in Figure 7.

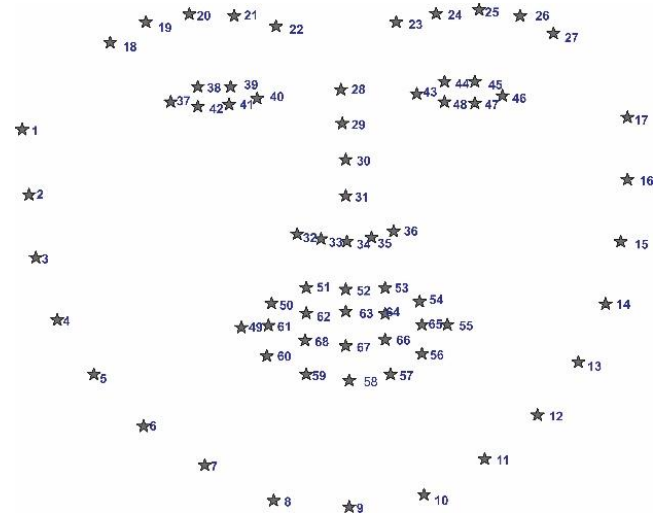


Figure 6. Facial landmarks on the human face

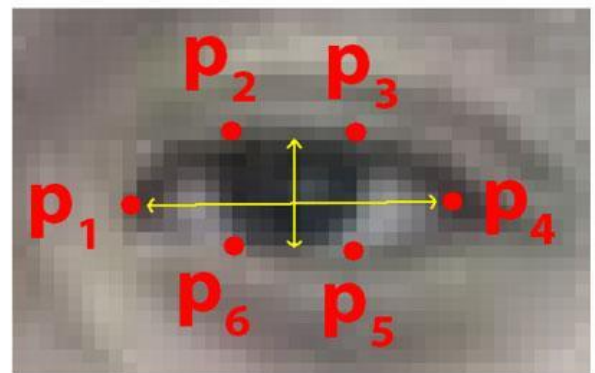


Figure 7. Eye detecting area on the human face

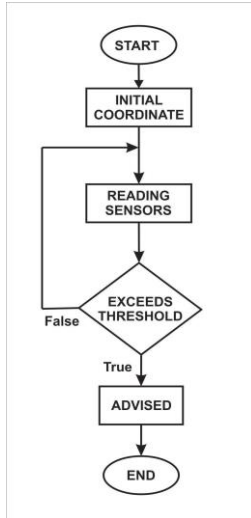
After extracting 6 points shown above, we apply a function called Eye Aspect Ratio (EAR). This is the core of the algorithm. The return value of this function is computed using this formula:

$$EAR = \frac{||p_2 - p_6|| + ||p_3 - p_5||}{2(||p_1 - p_4||)} \quad (2)$$

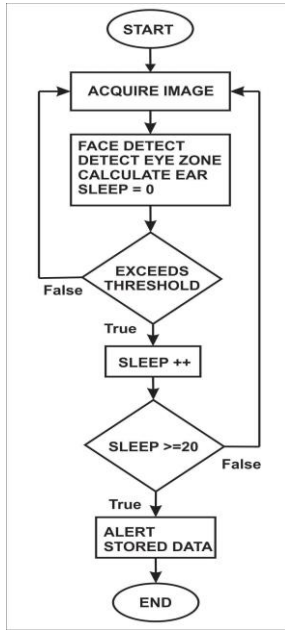
Each frame captured by the camera will be examined by the application, which will then compute the EAR for each frame and compare it with a fixed threshold of 0.25 pixels. When the eyelids are closing and the EAR is over the threshold, it is assumed that tiredness has been identified. The software will examine 20 frames in a sequence, and if they are all references to nodding off, it will determine that the user is going to enter a drowsy condition.

2.7 The algorithm

In order to make it easier to understand how the system works, we have designed algorithms to acquire body tilt data from gyroscope sensors as shown in Figure 8(a) and drowsiness detection from the camera as shown in Figure 8(b).



(a) Detect wrong posture



(b) Detect drowsy state

Figure 8. Detect wrong posture

3. EXPERIMENTS AND RESULTS

3.1 The 2.5 PM monitoring in the studying area

We ran an experiment for a week in a few specific locations throughout Hanoi to see how well the gadget could measure the concentration of particle matters. The characteristics from the provided Air Quality Index (AQI) map by website [56] are then compared to our data. The results are displayed in the Table 1 on an average basis:

The values that the sensor measured are close to those that are shown on the AQI map, as can be seen from the data above. In particular, the fine dust PM_{2.5} measurements' standard deviation is 2.1575 $\mu\text{g}/\text{m}^3$, and the fine dust PM₁₀ measurement's standard deviation is 6.375 $\mu\text{g}/\text{m}^3$. For PM_{2.5} and PM₁₀, respectively, this deviation translates to a difference of 3.9% and 2.8%.

Our system's threshold for dust concentration has been set at 35 $\mu\text{g}/\text{m}^3$. This is because the average dust concentration in our region has already exceeded the WHO criterion [57],

which was declared to be between 23 $\mu\text{g}/\text{m}^3$ and 51.2 $\mu\text{g}/\text{m}^3$ during August 2022. The outcomes of this experiment demonstrate the great accuracy with which our system can provide measurements, and users may rely on these results to determine the best ways to maintain a healthy environment and safeguard their health.

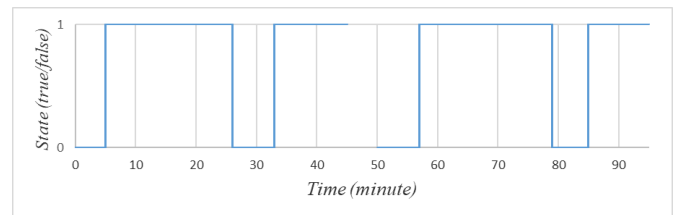
Table 1. Air quality examination

Location	AQI	AQI 2.5 $\mu\text{g}/\text{m}^3$	AQI 10 $\mu\text{g}/\text{m}^3$	Sys 2.5 $\mu\text{g}/\text{m}^3$	Sys 10 $\mu\text{g}/\text{m}^3$
Thanh Xuan	141	51.7	235	50	233
VNU	178	107.7	309	105	300
Linh Đam	91	31.1	135	30	133
Phuong Liet	104	36.7	161	35	159
U.S Embassy	137	50.1	227	50	225
Le Duan	151	55.5	255	55	253
Vuong Me	126	45.6	205	44	202

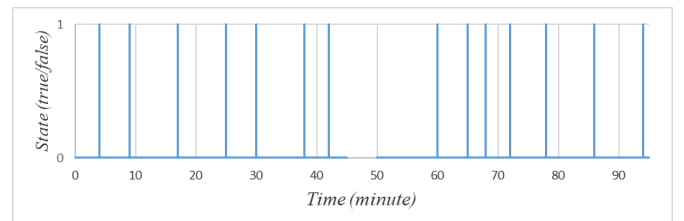
3.2 The habit of wrong sitting posture

In this section, we will present a comparison in monitoring students' sitting habits in the with and without the presence of device's alert method. The experiment was conducted as follows:

Ten pupils in a class, ranging in age from 6 to 10, were chosen at random to participate in the experiment. They were instructed to study for two 90-minute sessions, one in the morning and one in the afternoon of the same day, with a 5-minute break in between. We turned off the device's warning feature for the first session so that the children could sit in their natural posture. The findings of this experiment are documented in Figure 9(a). All of the device's features are turned on during the second session. As a result, every time a kid sits incorrectly, they will be informed and given the opportunity to adjust. The outcomes of this investigation are documented in Figure 9(b).



(a) With advice



(b) With advice

Figure 9. Posture status

As can be inferred from the data, there is an enormous difference between these two sessions as once applied the caution method and other was not.

In the first graph, the percentage of time the students sat in the correct posture only accounted for about 22.22% of the whole process. The average time students were able to hold the correct posture was about 5 to 7 minutes with only 4 times during the entire 90 minutes of study. In contrast, the majority of the time students were assessed as sitting in the wrong position, which was up to about 60 minutes. In comparison to the first graph, the second graph presents us with the exact opposite view. The student mostly maintained the proper sitting posture, with little or no retention in the incorrect positions. As you can see, the student readjusts back to the proper posture after being informed, roughly every 5 to 10 minutes while they are sitting incorrectly.

The results above have demonstrated the usefulness of the system in identifying the learner's sitting posture and assisting the student in upholding proper posture.

3.3 Testing on random pupils

We performed a study with 5 randomly selected kids, ages 8 to 10, at a primary school in Hanoi to evaluate the students' eye-to-desk distance habits and their ability to focus on learning while using the device. This is how the experiment was carried out, 6 sessions lasted 40 minutes and were divided equally between the morning and the afternoon of the same day for the students to complete.

In these lessons, students would practice answering the kinds of questions seen in History tests that they had never studied. As a result, at the conclusion of the class, a pre-designed exam would be administered to evaluate students' focus ability while using the device. The pupil who scored the highest on this test would get a gift.

The system was enabled, allowing the head-to-table distance measurement device and the wearable gadget that detects improper posture in students to work. 30 cm and 15 degrees were chosen as the threshold parameters. We keep track of how often students receive warnings in each lesson, and we've compiled that information in the Figure 10.

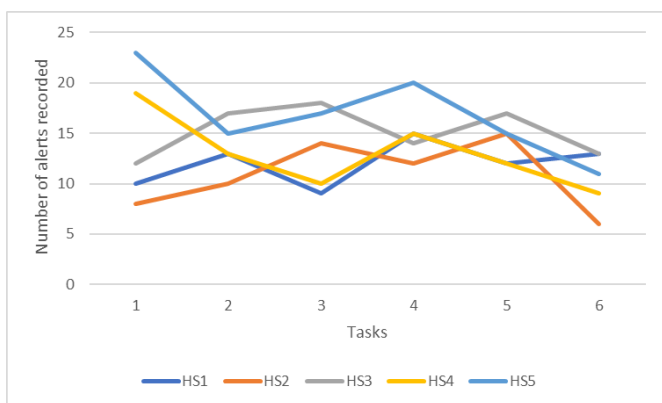


Figure 10. Number of alerts recorded in the experiment

As we can see, the graphs all have a tendency to fall off towards the conclusion of the period, and every student has been warned more than five times but no more than twenty-five times. The student with the greatest average number of errors out of the five that took part in the experiment is the fifth one down on the graph. After making 23 errors in the first

period, the student afterwards corrected his posture and stopped often slouching at the table. In period 4, the first session in the afternoon, the numbers for improper posture dropped to barely 15, then gradually increased to 20.

The fourth student's statistics followed the same pattern as the student above, but with lower values. Regarding the first and third-place kids, their scores varied throughout the course of the session but coincided at the conclusion with 13 errors. As the two eldest pupils, this demonstrates that they have been clinging onto a position that is all too comfortable to them, and altering it appears to be challenging.

Out of the five pupils, student 2 appears to have the fewest reported instances of poor posture. Although this student was able to sit upright and maintain her back straight, she frequently hunched down to write or read, which is why the cautions were given. The final exam results revealed that the kids' scores were generally between 7 and 9 on a scale of 10, with little variation amongst them. The pupil who scored the highest, was number 5 with nine points. This experiment showed that students learning new knowledge in a supervised environment of sitting posture gave positive results on the students' concentration assessment. In this experiment, aptitude was not taken into consideration; rather, the way a person sits and their ability to focus while studying in the presence of a gadget were the main concerns.

3.4 Calibrate camera angle

Sometimes we encounter unexpected outcomes when testing the system. The face is recognized by the computer, but the EAR is not as precise as the previous computation. Because of this, even if the youngster is still in a normal learning condition, the system misrepresents the child as being sleepy. As we have found out, the variation in α tilt angle, h height of the camera and the d distance from the sitting position to camera all contributed to the inaccuracy as shown in Figure 11. The student's height and the angle have no bearing on the outcome.

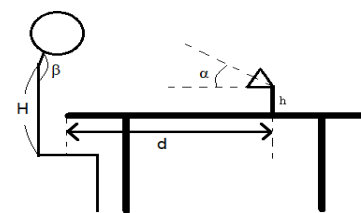


Figure 11. Calibrate camera angle view

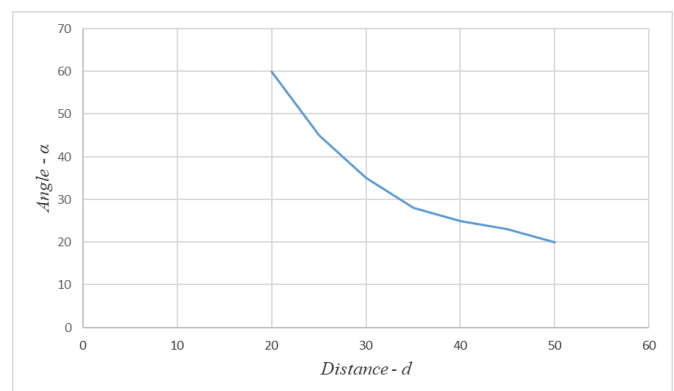


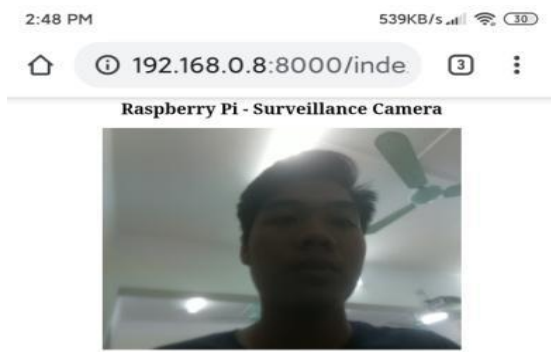
Figure 12. Depend on distance with camera angle view

We maintain the error-correcting values of h of 5 cm and EAR of 0.3. As long as the camera can detect and function properly, we adjust the distance d and assess α as shown in Figure 12.

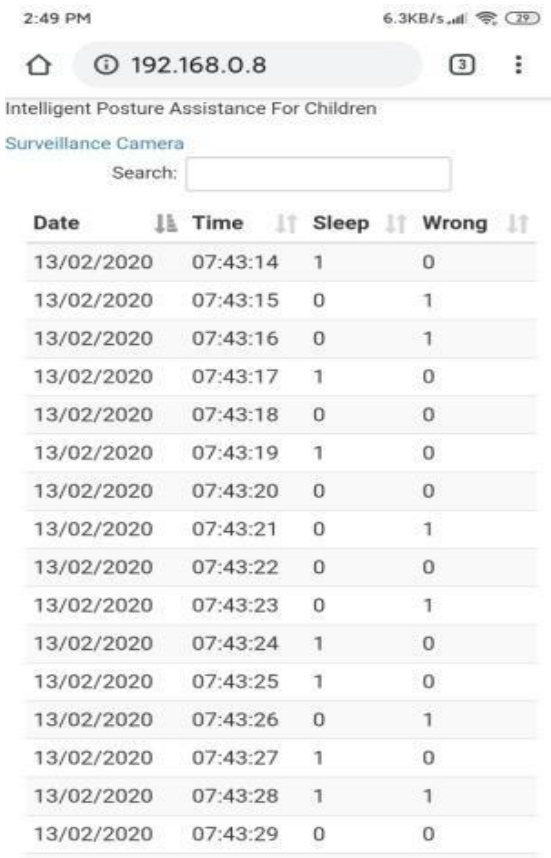
According to the graph, users should calibrate the system before usage to ensure that it operates as intended.

3.5 Data stored in Web server

We also gathered and stored information on the state of the student in the server to improve system performance. Their parents may find it useful to keep tabs on the kids. Therefore, based on their children's self-improvement, the parents may choose whether to keep using the gadget or cease shown in Figure 13(a) and in Figure 13(b) depict the website's front end and database, respectively.



(a) The front end of the website



(b) Database on server

Figure 13. Website management interface

4. CONCLUSIONS

In this project, we successfully built a system with a variety of integrated features. Including tools to keep kids in the right posture, detect them dozing off in class, keep an eye on the amount of fine dust in the classroom, and even a website for parents to keep an eye on kids. Four experiments were run as part of this research to evaluate the system's functionality. First, in experiments 2 and 3, we evaluated the device's capacity to support users in maintaining a straight back, with experiment 3 focusing on how the device affected the ability of the user to focus. The fine dust concentration meter's accuracy is tested, and positive findings are obtained when comparing the measured data to the AQI values that have been published. The fourth experiment presents a method for detecting doze. In order for users to configure the camera themselves in accordance with their usage circumstances, we have also supplied instructions for doing so. Later, the website's user interface that displays the children's data was also introduced. Our system currently has more integrated functionality than many other systems, per the evaluation. Additionally, the functionalities have shown to be quite accurate and will probably get an improvement in the future. We are certain that this system is completely functional for everyday usage and it not only can make a significant contribution to helping kids maintain proper sitting posture while also assisting them in staying focused during the learning process. Last but not least, one of the projects we are working on involves the creation of computer vision algorithms, which can be used to track psychological behavior statistics in elementary school students using this device.

REFERENCES

- [1] Yin, X.Q., Wang, L.L., Zhang, L. (2022). Skeletal structure and training adaptability of athletes based on biomechanical analysis. *Journal of Healthcare Engineering*, 2022: 3083821. <https://doi.org/10.1155/2022/3083821>
- [2] Stefan, S., Katelyn, A.B., Brett, T.A., Daniel, G., Dennis E.A. (2020). Musculoskeletal full-body models including a detailed thoracolumbar spine for children and adolescents aged 6-18 years. *Journal of Biomechanics*, 102: 109305. <https://doi.org/10.1016/j.jbiomech.2019.07.049>
- [3] Salameh, M.A., Boyajian, S.D., Odeh, H.N., Amaireh, E.A., Funjan, K.I., Al-Shatanawi, T.N. (2022). Increased incidence of musculoskeletal pain in medical students during distance learning necessitated by the COVID-19 pandemic. *Clinical Anatomy*, 35(4): 529-536. <https://doi.org/10.1002/ca.23851>
- [4] Schwertner, D.S., da Silva Oliveira, R.A.N., Swarowsky, A., Felden, É.P.G., Beltrame, T.S., da Luz Koerich, M.H.A. (2022). Young people's low back pain and awareness of postural habits: A cross-sectional study. *Journal of Back and Musculoskeletal Rehabilitation*, 35(5): 983-992. <https://doi.org/10.3233/bmr-200356>
- [5] Zaheer, M., Fatima, N., Riaz, U., Haseeb, N. (2022). Association of heavy bag lifting time with postural pain in secondary school students. *Pakistan BioMedical Journal*, 5(2): 64-67. <https://doi.org/10.54393/pbmj.v5i2.232>
- [6] Patterson, E., Brown, E., Ruminiski, C., Miller, T. (2021).

- Electronics: The enemy of posture and how to protect yourself. *Front Young Minds*, 9: 553496. <http://doi.org/10.3389/frym.2021.553496>
- [7] Lee, S.P., Hsu, Y.T., Bair, B., Toberman, M., Chien, L.C. (2018). Gender and posture are significant risk factors to musculoskeletal symptoms during touchscreen tablet computer use. *Journal of Physical Therapy Science*, 30(6): 855-861. <https://doi.org/10.1589/jpts.30.855>
- [8] Lei, Y., Xinhai, L., Bin, Y., Yeen, H. (2020). Prevalence of incorrect posture among children and adolescents: Finding from a large population-based study in China. *iScience*, 23(5). <https://doi.org/10.1016/j.isci.2020.101043>
- [9] Kounter, T. (2019). The prevalence and consequences of poor posture in children and adolescents. *Senior Honors Theses*, 903. <https://digitalcommons.liberty.edu/honors/903>
- [10] Voichyshyn, L., Golod, N., Marchuk, O., Zastavna, O., Chepurna, L., Rybalko, P., Khomenko, S., Kuzmik, V., Kolisnyk, S., Babii, I. (2022). Physical rehabilitation of adolescents with postural disorders in the sagittal plane and its relation to neurophysiology. *BRAIN. Broad Research in Artificial Intelligence and Neuroscience*, 13(1): 61- 87. <https://doi.org/10.18662/brain/13.1/269>
- [11] Analyn, D.P., Rexomar, D.P. (2022). Motivational strategies of teacher in relation to learner's academic performance. *International Journal of Multidisciplinary Research and Analysis*, 5(1). <https://doi.org/10.47191/ijmra/v5-i1-28>
- [12] Kamal, G., Raja, S.K.B., Dhiraj, K., Sunil, L.B., Neeraj C., Saravanan, G. (2022). A review paper on wireless sensor network techniques in Internet of Things (IoT), *Materials Today*, 51(1): 161-165. <https://doi.org/10.1016/j.matpr.2021.05.067>
- [13] Wei, J. (2022). Design of intelligent perception module based on wireless sensor network and basketball sports attitude. *Wireless Communications and Mobile Computing*, 2022: 8227604. <https://doi.org/10.1155/2022/8227604>
- [14] Takasaki, H. (2017). Habitual pelvic posture and time spent sitting: Measurement test-retest reliability for the LUMOback device and preliminary evidence for slouched posture in individuals with low back pain. *SAGE Open Medicine*. <https://doi.org/10.1177/2050312117731251>
- [15] Airaksinen, M., Räsänen, O., Ilén, E., Häyrynen, T., Kivi, A., Marchi, V., Gallen, A., Blom, S., Varhe, A., Kaartinen, N., Haataja, L., Vanhatalo, S. (2020). Automatic posture and movement tracking of infants with wearable movement sensors. *Sci Rep.*, 10: 169. <https://doi.org/10.1038/s41598-019-56862-5>
- [16] Bi, X. (2021). Infrared sensors and ultrasonic sensors. In: *Environmental Perception Technology for Unmanned Systems. Unmanned System Technologies*. Springer, Singapore, 143-176. https://doi.org/10.1007/978-981-15-8093-2_5
- [17] Rosa, M.S., Mateusz, J., Sergio, L., José, M.G., Norberto, L.G. (2019). Novel method of remotely monitoring the face-device distance and face illuminance using mobile devices: A pilot study. *Journal of Ophthalmology*, 2019: 1946073. <https://doi.org/10.1155/2019/1946073>
- [18] Baird, P.N., Saw, S.M., Lanca, C. et al. (2020). Myopia. *Nature Reviews Disease Primers*, 6: 99. <https://doi.org/10.1038/s41572-020-00231-4>
- [19] Khabarlak, K., Koriashkina, L. (2022). Fast facial landmark detection and applications: A survey. *Journal of Computer Science & Technology*, 22(1): 12-41. <https://doi.org/10.48550/arXiv.2101.10808>
- [20] Jun, H.J., Byung, W.J, Jung, H.K., Sung, J.K., Woon, Y.H. (2020). Development of an IoT-Based indoor air quality monitoring platform. *Journal of Sensors*, 2020: 8749764. <https://doi.org/10.1155/2020/8749764>
- [21] Singer, B.C., Delp, W.W. (2018). Response of consumer and research grade indoor air quality monitors to residential sources of fine particles. *Indoor Air*, 28(4): 624-639. <https://doi.org/10.1111/ina.12463>
- [22] Qihong, D., Linjing, D., Yufeng, M., Xilong, G., Yuguo, L. (2019). Particle deposition in the human lung: Health implications of particulate matter from different sources. *Environmental Research*, 169: 237-245. <https://doi.org/10.1016/j.envres.2018.11.014>
- [23] InvenSense Inc. MPU-6000 and MPU-6050 Register Map and Descriptions Revision 4.2, datasheet. <https://invensense.tdk.com>, accessed on Aug. 2, 2022.
- [24] Nordic Semiconductor.Inc. nRF24L01 Single Chip 2.4GHz Transceiver Product Specification, datasheet. <https://www.nordicsemi.com>, Accessed Aug. 2, 2022.
- [25] Xu, Y., Luo, W., Zhang, L. (2018). Research on control system of quadrotor based on ADRC. *Chinese Control and Decision Conference*. <https://doi.org/10.1109/CCDC.2018.8407631>
- [26] Kemper, S. (2020). Tremolo-Harp: A Vibration-Motor Actuated Robotic String Instrument. In *Proceedings of the International Conference on New Interfaces for Musical Expression*, 301-304. https://www.nime.org/proceedings/2020/nime2020_paper57.pdf
- [27] Sharp.Inc, GP2Y0A21YK0F, datasheet. <https://global.sharp>, accessed on Aug. 2, 2022.
- [28] Atmel Inc, Atmega8, datasheet. <https://www.microchip.com>, accessed on July 27, 2022.
- [29] Feng, D., Lu, C., Cai, Q., Lu, J. (2022). A study on the design of vision protection products based on children's visual fatigue under online learning scenarios. *Healthcare*, 10(4): 621. <https://doi.org/10.3390/healthcare10040621>
- [30] Sharp.Inc, GP2Y1010AU0F, datasheet. <https://global.sharp>, accessed on Aug. 2, 2022.
- [31] "LCD-MODULE 2x16", datasheet.
- [32] Raspberry Pi 3, <https://www.raspberrypi.org>, accessed on July 22, 2022.
- [33] Philipp, K., Derek, B., Thabo, B., Markus, G. (2019). Analysis and improvement of facial landmark detection. *Technical Report*. <https://doi.org/10.13140/RG.2.2.10980.42886>
- [34] Guo, X.J., Li, S.Y., Yu, J.K., Zhang, J.W., Ma, J.Y., Ma, L., Liu, W., Ling, H.B. (2019) PFLD: A practical facial landmark detector. *ArXiv*. <https://doi.org/10.48550/arXiv.1902.10859>
- [35] "Dlib", <http://dlib.net>, accessed on Aug. 2, 2022
- [36] Priadana, A., Habibi, M. (2019). Face detection using Haar Cascades to filter selfie face image on instagram. *International Conference of Artificial Intelligence and Information Technology (ICAIIIT)*, Yogyakarta, Indonesia. <https://doi.org/10.1109/ICAIIIT.2019.8834526>
- [37] Tyas Purwa Hapsari, D., Gusti Berliana, C., Winda, P., Arief Soeleman, M. (2018). Face detection using Haar

- Cascade in difference illumination. International Seminar on Application for Technology of Information and Communication, Semarang, Indonesia. <https://doi.org/10.1109/ISEMANTIC.2018.8549752>
- [38] Rohadi, E., Suwignjo, S.A., Pradana, M.C., Setiawan, A., Siradjuddin, I., Ronilaya, F., Amalia, Asmara, R.A., Ariyanto, R. (2018). Internet of Things: CCTV Monitoring by Using Raspberry Pi. International Conference on Applied Science and Technology, Manado, Indonesia, 454-457. <https://doi.org/10.1109/iCAST1.2018.8751612>
- [39] Tanvir, S. (2020). Microelectromechanical system. Projects: Training of PhD students and young researchers in peer review of papers - Registration on PUBLONS ACADEMY Artificial Intelligence Nanoactuator design selection by system based approach RG Achievement and Accomplishments Achievements, Accomplishments and Scholarly Contributions Certificates of Achievement, Accomplishment, Reviewing and Participation RG Achievement Measuring of scientific productivity of researchers at Quisqueya University on ResearchGate. <http://dx.doi.org/10.13140/RG.2.2.27193.60008>
- [40] Mohammed, Z., Elfadel, I.M., Rasras, M. (2018). Monolithic multi degree of freedom (MDoF) capacitive MEMS accelerometers. *Micromachines*, 9(11): 602. <https://doi.org/10.3390/mi9110602>
- [41] Zhang, H., Zhang, C., Chen, J., Li, A. (2022). A Review of symmetric silicon MEMS gyroscope mode-matching technologies. *Micromachines*, 13(8): 1255. <https://doi.org/10.3390/mi13081255>
- [42] Kwon, H.J, Seok, S., Lim, G. (2017). System modeling of a MEMS vibratory gyroscope and integration to circuit simulation. *Sensors*, 17(11): 2663. <https://doi.org/10.3390/s17112663>
- [43] Zhao, Y., Zhao, J., Xia, G.M., Qiu, A.P., Su, Y., Wang, X., Xu, Y.P. (2015). A $0.57^\circ/\text{h}$ bias instability $0.067^\circ/\sqrt{\text{h}}$ angle random walk MEMS gyroscope with CMOS readout circuit. Asian Solid-State Circuits Conference, Xiamen, China. <https://doi.org/10.1109/ASSCC.2015.7387505>
- [44] Zhang, W. (2021). Research on QMEMS gyro drift processing method based on adaptive Kalman filter. IEEE 15th International Conference on Electronic Measurement & Instruments, Nanjing, China, pp. 324-328. <https://doi.org/10.1109/ICEMI52946.2021.9679555>
- [45] Minh, L.H., Antonio, P. (2021). Yaw/Heading optimization by drift elimination on MEMS gyroscope, *Sensors and Actuators A: Physical*, 325: 112691. <https://doi.org/10.1016/j.sna.2021.112691>
- [46] Chungag, A., Engwa, G.A., Sewani-Rusike, C.R., Nkeh-Chungag, B.N. (2021). Effect of seasonal variation on the relationship of indoor air particulate matter with measures of obesity and blood pressure in children. *Journal of Health & Pollution*, 11(30): 210610. <https://doi.org/10.5696/2156-9614-11.30.210610>
- [47] Javeria, Z., Jongho, J., Seung-Bok, L., Jin, S.K. (2018). Effect of particulate matter on human health, prevention, and imaging using PET or SPECT. *Progress in Medical Physics*, 29(3): 81-91. <https://doi.org/10.14316/pmp.2018.29.3.81>
- [48] Mohammad, G., Cinna, S., Pablo, R., William, A.G., Vladislav, K. (2022). Laboratory and field evaluation of three low-cost particulate matter sensors. *IET Wireless Sensor Systems*, 12(1): 21-32. <https://doi.org/10.1049/wss2.12034>
- [49] Shree, V.G., Krishna, R.P.M., Srinivasa, K.G. (2021). Framework and method for measurement of particulate matter concentration using low cost sensors. *International Journal of Advanced Computer Science and Applications (IJACSA)*, 12(12). <http://dx.doi.org/10.14569/IJACSA.2021.01212103>
- [50] Yang, X., Shen, Y. (2018). Sitting posture correction device based on infrared distance measurement. IEEE International Conference on Real-Time Computing and Robotics. <https://doi.org/10.1109/RCAR.2018.8621764>
- [51] OpenCV. <https://opencv.org>, accessed on Aug. 2, 2022.
- [52] Kalangi, R.R, Maloji, S., Sundar, P.S., Ahammad, S.H. (2022). Deployment of Haar Cascade algorithm to detect real-time faces. The 4th International Conference on Smart Systems and Inventive Technology, Tirunelveli, India, pp. 1676-1680. <https://doi.org/10.1109/ICSSIT53264.2022.9716530>
- [53] Alankar, B., Ammar, M.S., Kaur, H. (2021). Facial Emotion Detection Using Deep Learning and Haar Cascade Face Identification Algorithm. In: Das, S., Mohanty, M.N. (eds) *Advances in Intelligent Computing and Communication. Lecture Notes in Networks and Systems*, vol 202. Springer, Singapore. https://doi.org/10.1007/978-981-16-0695-3_17
- [54] Viola, P., Jones M. (2001). Rapid object detection using a boosted Cascade of simple features. Accepted Conference on Computer Vision and Pattern Recognition 2001. <https://cse.buffalo.edu/~jcorso/t/555pdf/ViJoCVPR2001.pdf>
- [55] Kazemi, V., Sullivan, J. (2014). One millisecond face alignment with an ensemble of regression trees. *Computer Vision and Pattern Recognition*, Columbus, OH, USA. <https://doi.org/10.1109/CVPR.2014.241>
- [56] AQI map, <https://aqicn.org/map/hanoi/vn>, accessed on Sep. 5 to 10, 2022.
- [57] World Health Organization. (2021). WHO global air quality guidelines: particulate matter (PM_{2.5} and PM₁₀), ozone, nitrogen dioxide, sulfur dioxide and carbon monoxide. World Health Organization. <https://apps.who.int/iris/handle/10665/345329>, accessed on Aug. 2, 2022.